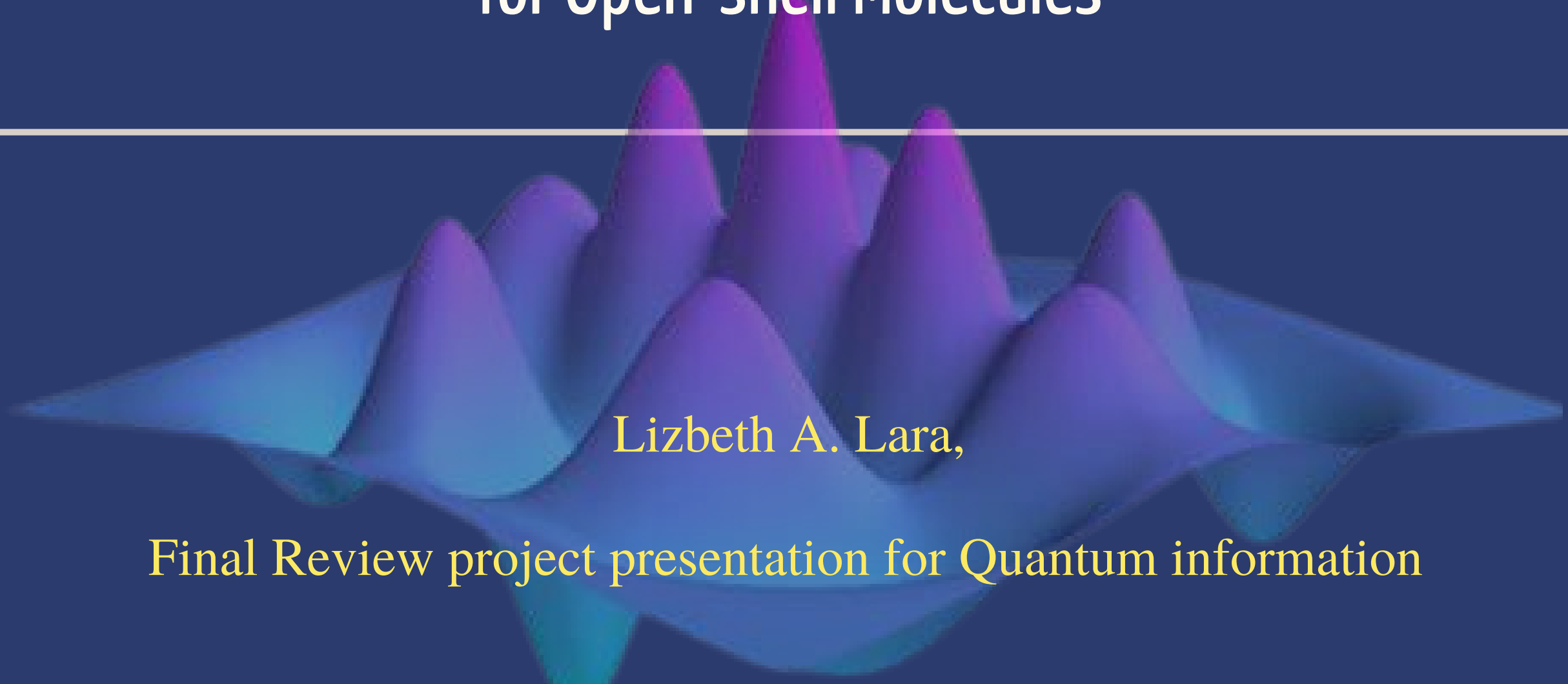


# Quantum Entanglement Implementation in Energy Gaps Computation for Open-shell Molecules

---



A 3D surface plot on a dark blue background, showing a series of peaks and valleys in shades of purple and blue, representing energy gap calculations for molecules.

Lizbeth A. Lara,

Final Review project presentation for Quantum information

Final Presentation Event

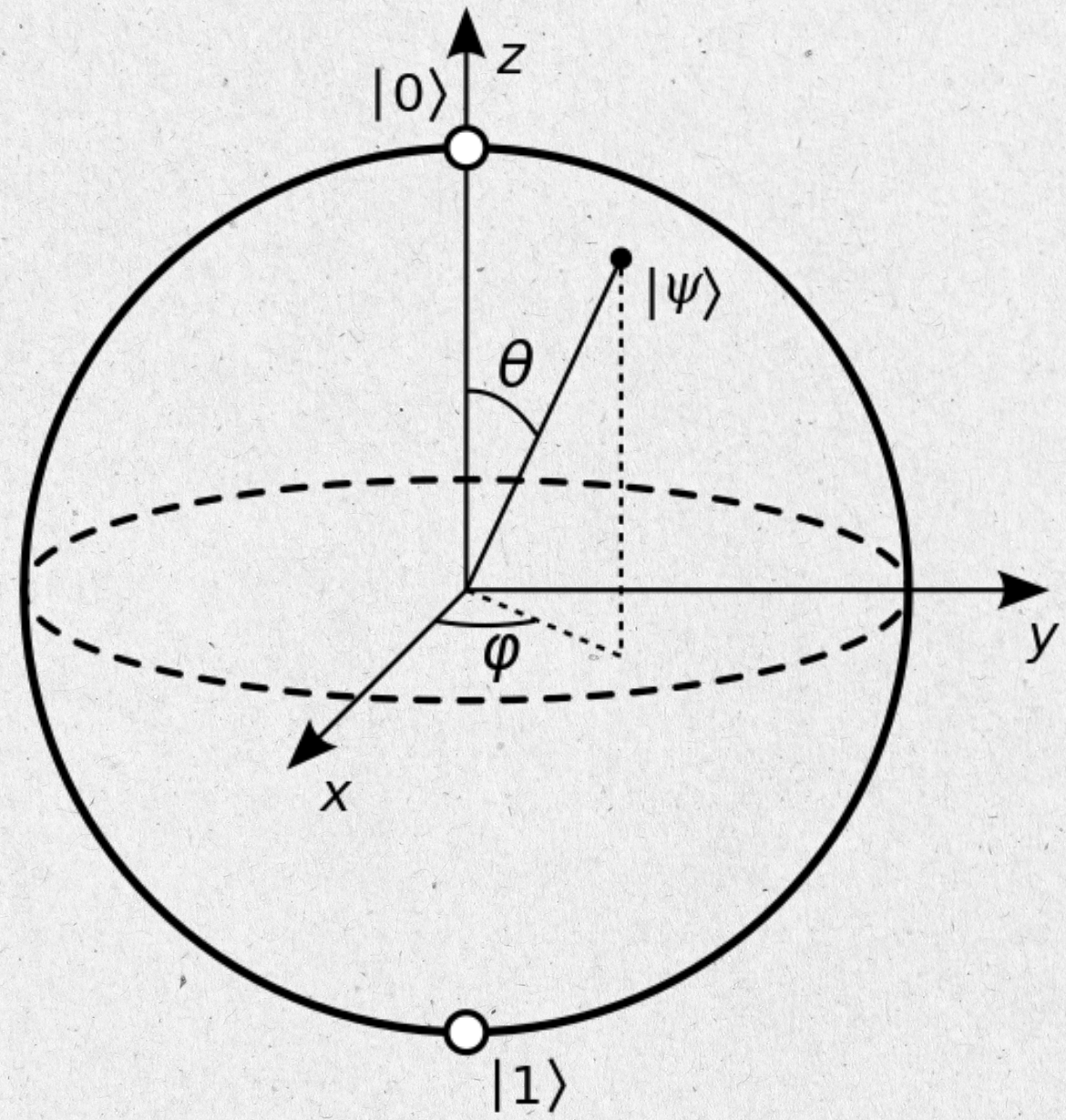
June 06, 2024



SCHOOL OF  
PHYSICAL SCIENCES  
AND NANOTECHNOLOGY

UNIVERSIDAD  
**YACHAY**  
TECH 

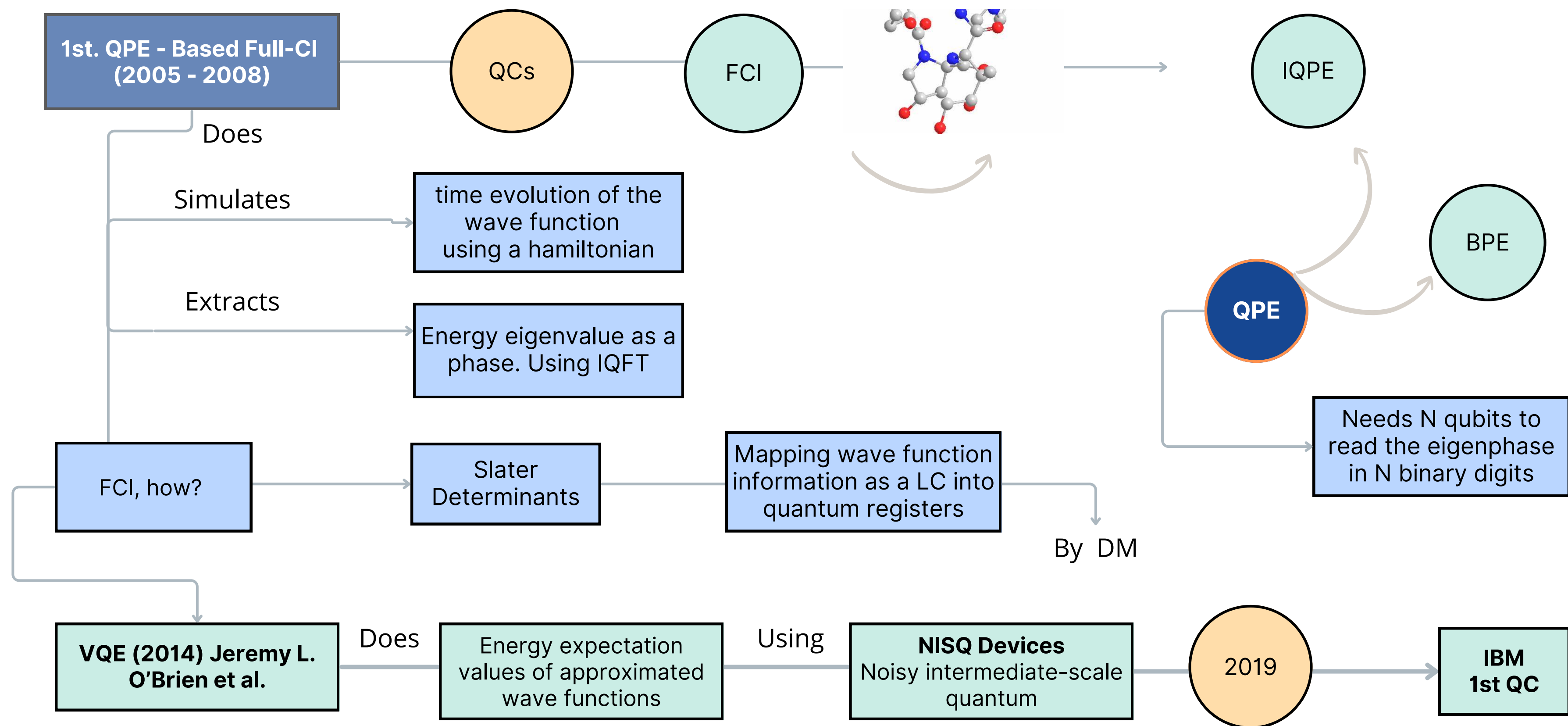
# Importance



- Huge range of applications. Disrupt the fields of computational and materials chemistry.
- Understanding in atomic and molecular systems.
- optimization in quantum mechanical systems simulations.
- free from controlled time and convergence does not depend on the system size.
- Understanding quantum machine learning.



## Development context throughout the history



## Open - shell systems

Open shell refers to a **valence shell** that is **not completely filled** with electrons or has **not given all of its valence electrons** through chemical bonds with other atoms or molecules during a chemical reaction.

Open-shell (radical character) systems have one or more unpaired electrons. These **unpaired electrons** lead to **unique electronic structures, and properties**. Applications : photodetectors, spintronics

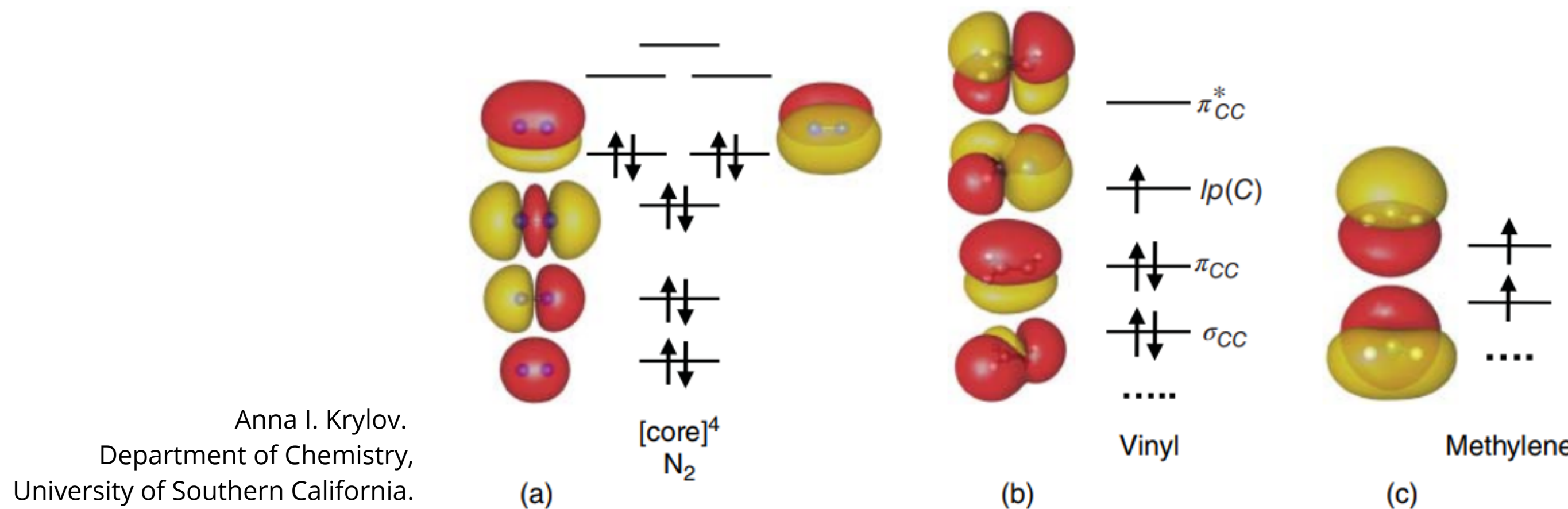


Fig 1. a) closed shell molecule, b) and c) are examples of open shell molecules, radical and diradical.

## Wave function mapping based on the Jordan–Wigner transformation (JWT)

In the JWT, each qubit stores the occupancy of a particular spin orbital: the qubit is in the  $|1\rangle$  state if the spin orbital is occupied by an electron, otherwise  $|0\rangle$

It is useful to map a fermionic Hamiltonian into a spin Hamiltonian. A series of spins is equivalent to a chain of qubits for quantum computing and viceversa.

$$S_j^- = \exp\left(i\pi \sum_{l=1}^{j-1} f_l^\dagger f_l\right) f_j$$

$$S_j^+ = f_j^\dagger \exp\left(-i\pi \sum_{l=1}^{j-1} f_l^\dagger f_l\right)$$

$$S_j^Z = f_j^\dagger f_j - \frac{1}{2}$$

## Wave function mapping based on the Jordan–Wigner transformation (JWT)

A Hamiltonian for the systems under study is written in the second quantised formula as in eq. 7,

$$H = \underbrace{\sum_{p,q} h_{pq} a_p^\dagger a_q}_{T+U} + \frac{1}{2} \underbrace{\sum_{p,q,r,s} h_{pqrs} a_p^\dagger a_q^\dagger a_r a_s}_V \quad (7)$$

where  $a_p^\dagger$  and  $a_p$  are creation and annihilation operators, respectively, acting on the  $p$ -th spin orbital.

As a result, the molecular Hamiltonian in eqn. (7) is transformed to the qubit Hamiltonian consisting of a linear combination of **Pauli strings**, as in eqn (10) and (11).

$$H = \sum_{p,q} h_{pq} a_p^\dagger a_q + \frac{1}{2} \sum_{p,q,r,s} h_{pqrs} a_p^\dagger a_q^\dagger a_r a_s \quad (7)$$

$$a_p^\dagger = \frac{1}{2} (X_{\textcolor{brown}{p}} - i Y_{\textcolor{blue}{p}}) \otimes \prod_{u=1}^{p-1} Z_u \quad (8)$$

$$a_p = \frac{1}{2} (X_{\textcolor{brown}{p}} + i Y_{\textcolor{blue}{p}}) \otimes \prod_{u=1}^{p-1} Z_u \quad (9)$$

$$H = \sum_m w_{\textcolor{brown}{m}} P_m \quad (10)$$

In the JWT,  $a_p^\dagger$  and  $a_p$  are transformed to the products of Pauli operators (Pauli strings) using eqn (8) and (9),

$$H = \sum_{p,q} h_{pq} a_p^\dagger a_q + \frac{1}{2} \sum_{p,q,r,s} h_{pqrs} a_p^\dagger a_q^\dagger a_r a_s \quad (7)$$

$$a_p^\dagger = \frac{1}{2} (X_{\textcolor{brown}{p}} - i Y_{\textcolor{blue}{p}}) \otimes \prod_{u=1}^{p-1} Z_u \quad (8)$$

$$a_p = \frac{1}{2} (X_{\textcolor{brown}{p}} + i Y_{\textcolor{blue}{p}}) \otimes \prod_{u=1}^{p-1} Z_u \quad (9)$$

$$H = \sum_m w_{\textcolor{brown}{m}} P_m \quad (10)$$

Wave function mapping based on the Jordan–Wigner transformation  
(JWT)

$$P_{\textcolor{brown}{m}} = \sigma_{N\text{SO}} \otimes \sigma_{N\text{SO}-1} \otimes \dots \otimes \sigma_1, \quad \sigma_k \in \{I, X, Y, Z\} \quad (11)$$

By applying Trotter–Suzuki decomposition, the time evolution operator  $\exp(-iHt)$  becomes products of the exponential of Pauli strings (eqn. 12):

$$\exp(-iHt) \approx \left[ \prod_{\textcolor{brown}{m}} \exp(-iw_{\textcolor{brown}{m}} P_{\textcolor{brown}{m}} t/N) \right]^N \quad (12)$$

## Entanglement

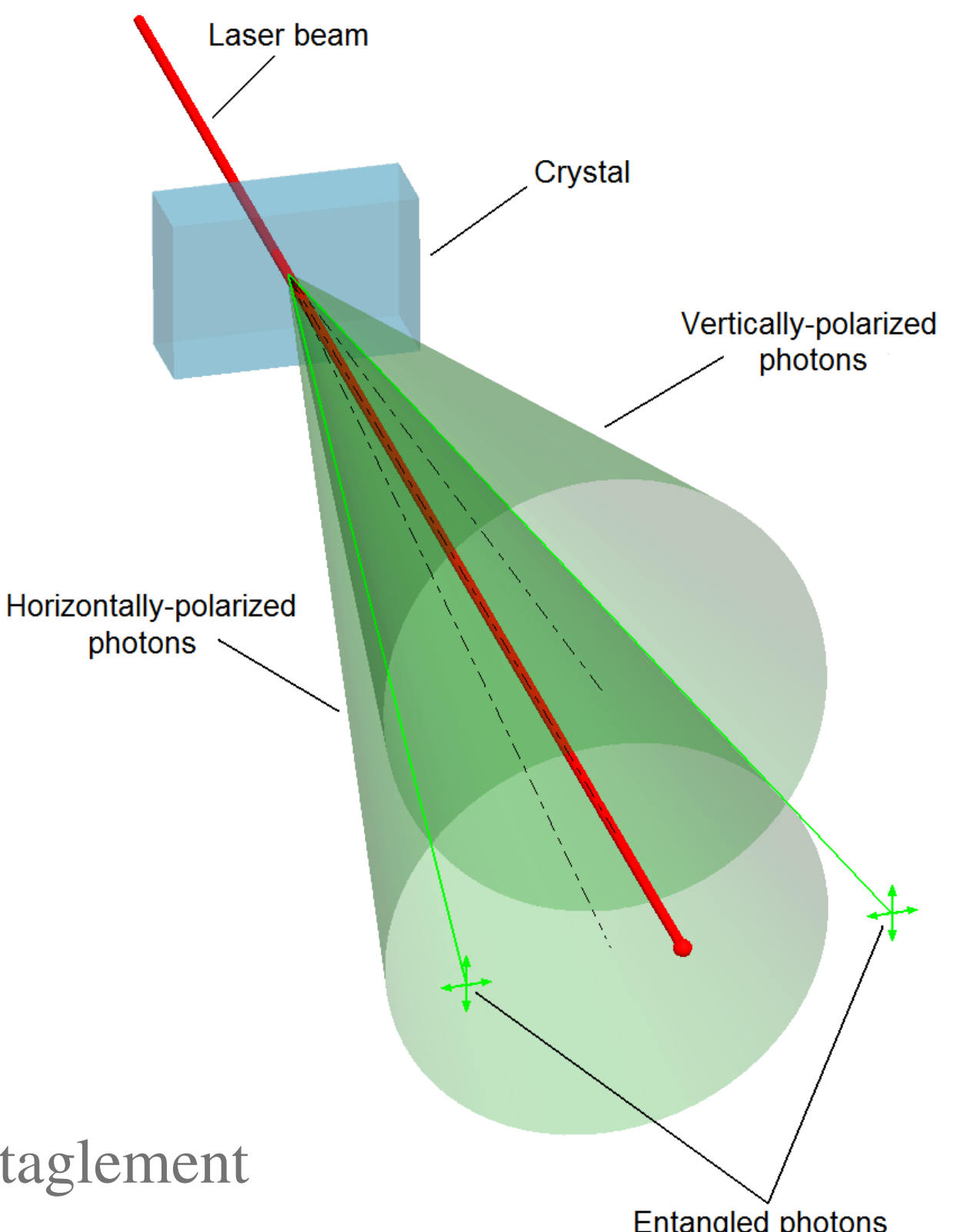
Entanglement is a quantum phenomenon that occurs when **two particles interact and become linked together.**

This link allows them to **share properties and influence each other**, even if they are separated by a large distance.

It has been described as “spooky action at a distance” because the **particles are able to interact without any physical connection.**

Entanglement works by linking two qubits together in such a way that the state of one is dependent on the state of the other

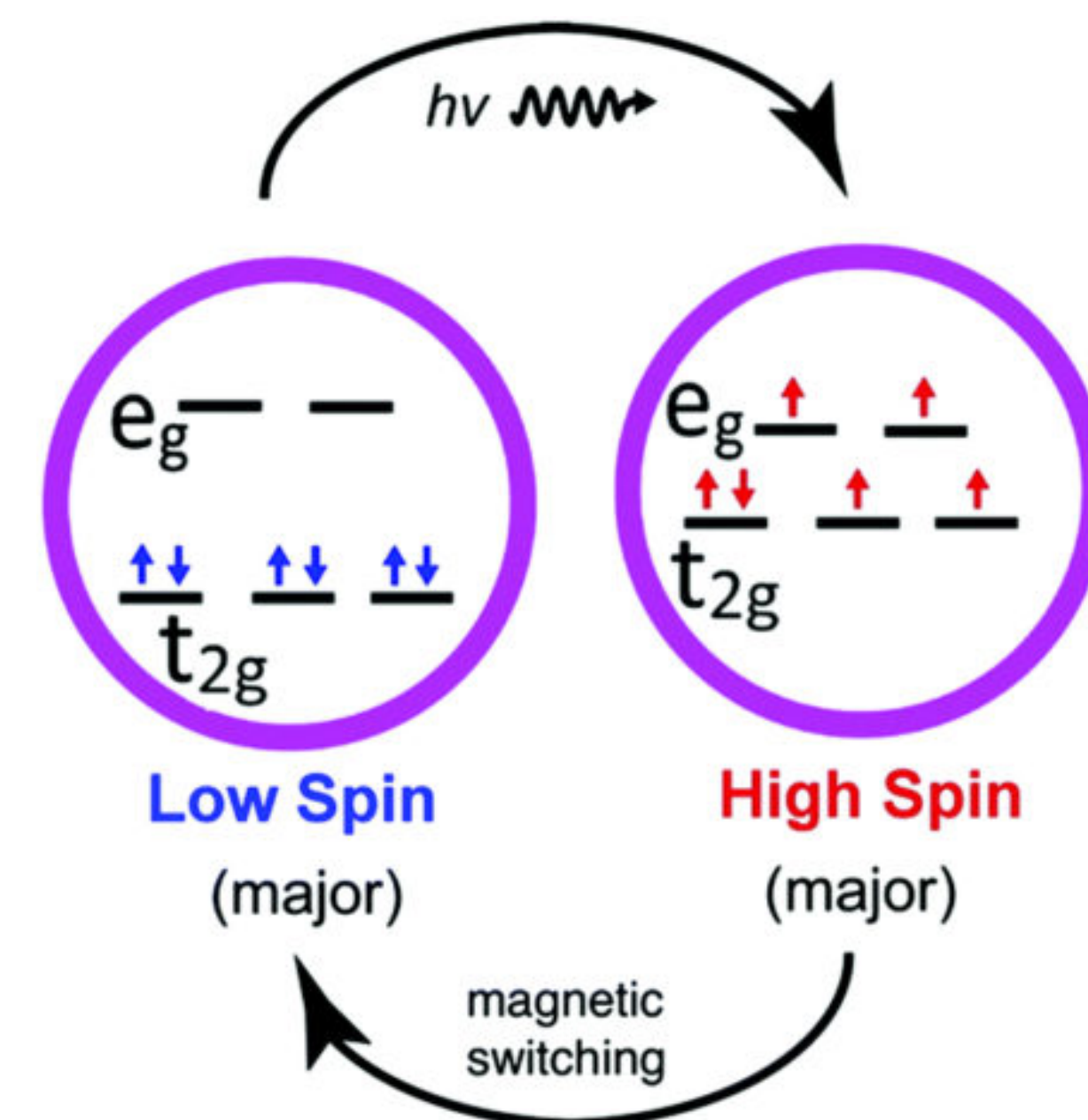
Fig. 2 Entaglement



If the splitting is small, the electrons can spread out over both levels (a high-spin state).

For some classes of molecules, transitions from low- to high-spin states (and vice versa) can be triggered.

This “spin crossover” phenomenon is a promising functionality that may be suitable for application in molecular spintronic devices.



From Berkeley Lab, (April 07, 2018).  
<https://als.lbl.gov/toward-control-spin-states-molecular-electronics/>

Fig. 3 transition from low to high spin and viceversa.

## BXB Algorithm for the direct calculation of spin state energy gaps

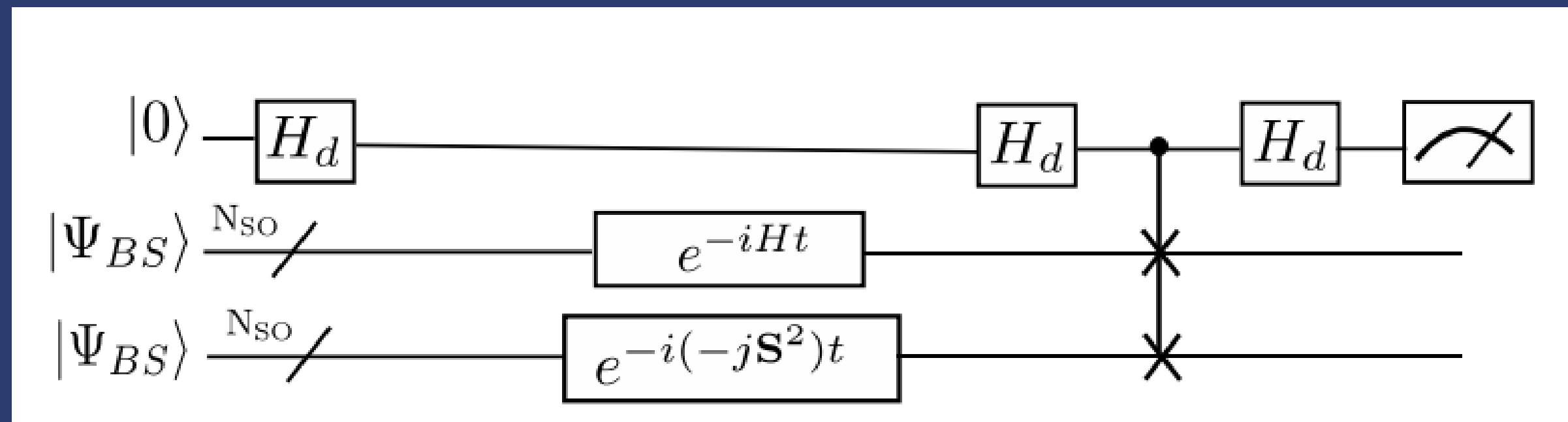


Fig. 4 A quantum circuit for the BXB algorithm. Adapted from (Sugisaki, 2021)

'Bayesian exchange coupling parameter calculator with broken-symmetrywave functions

## BPE Algorithm

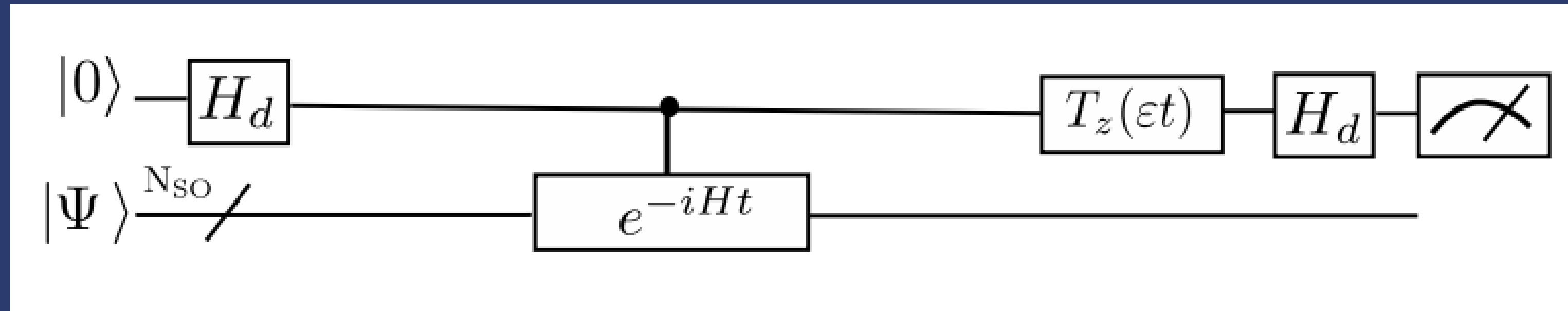


Fig. 5 A quantum circuit for the BPE algorithm. Adapted from (Sugisaki, 2021)

it uses only one ancillary qubit, to estimate the phase corresponding to an eigenvalue of a given unitary operator.

## Bayesian Phase Difference Estimation (BPDE ) Algorithm

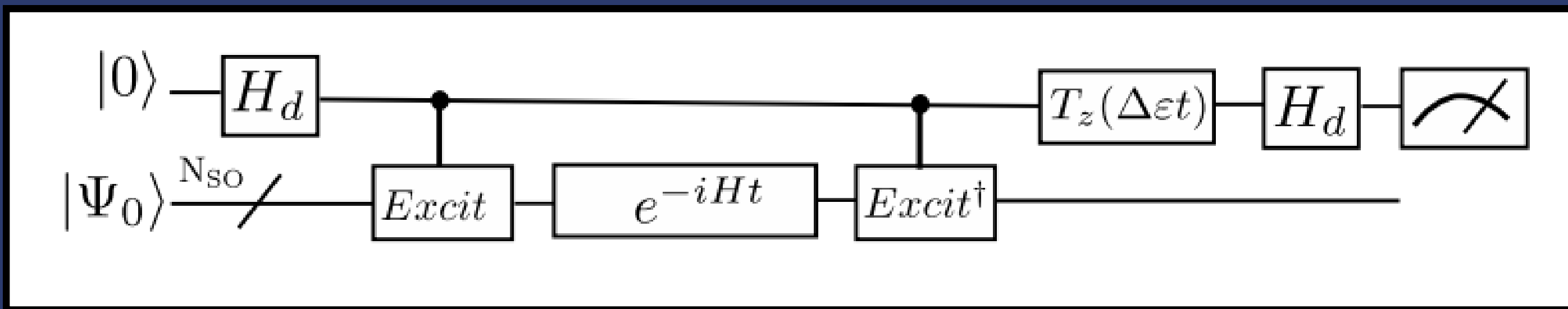


Fig. 6 A quantum circuit for the BPDE algorithm. Adapted from (Sugisaki, 2021)

# Bayesian Phase Difference Estimation (BPDE ) Algorithm

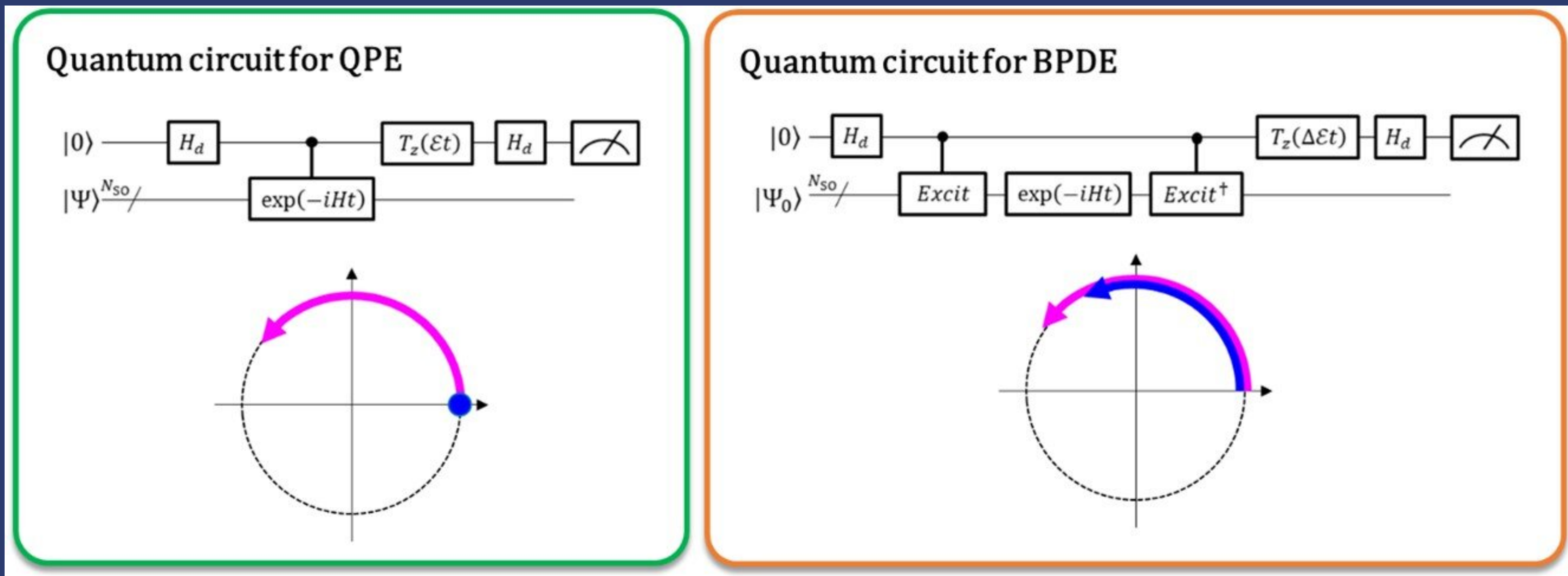


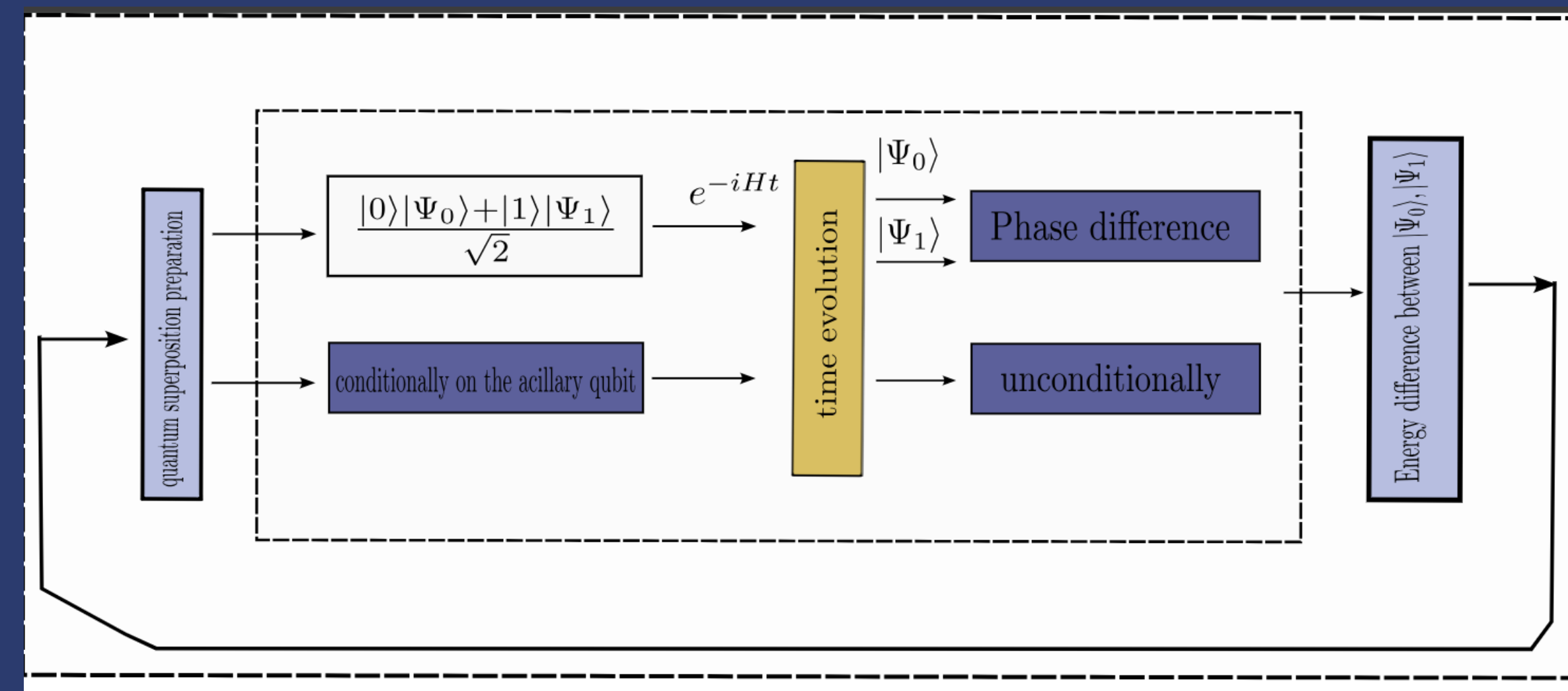
Fig. 7 Comparison of the phase difference computation in QPE and BPDE algorithms (Sugisaki, 2021)

by Osaka City University, 2021.  
<https://phys.org/news/2021>

## Bayesian Phase Difference Estimation (BPDE ) Algorithm

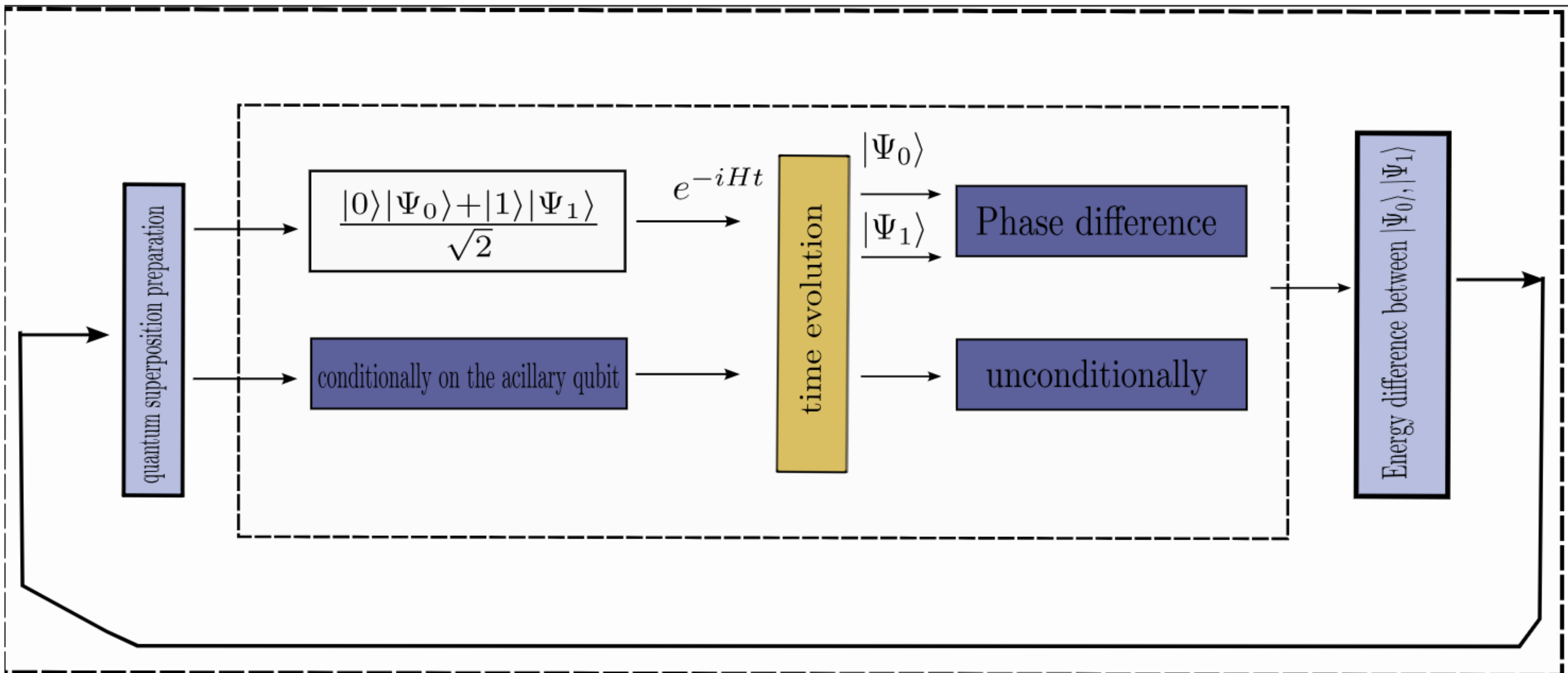
aim: to calculate the difference in energy between two quantum states directly. Specifically, it focuses on energy gaps between electronic states. i.e., calculate the difference of two eigenphases of unitary operators.

### How BPDE Works:



This approach allows for efficient energy gap calculations, making it promising for quantum chemistry problems.

## How BPDE Works:



This approach allows for efficient energy gap calculations, making it promising for quantum chemistry problems.

## Bayesian Phase Difference Estimation (BPDE ) Algorithm

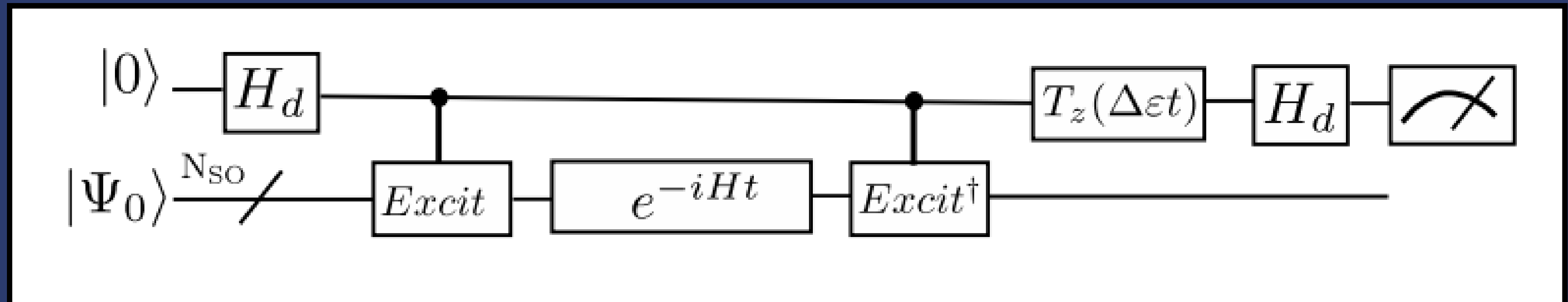


Fig. 8 A quantum circuit for the BPDE algorithm. Adapted from (Sugisaki, 2021)

## Vertical ionization energies from the quantum circuit simulations and those from the CAS-CI.

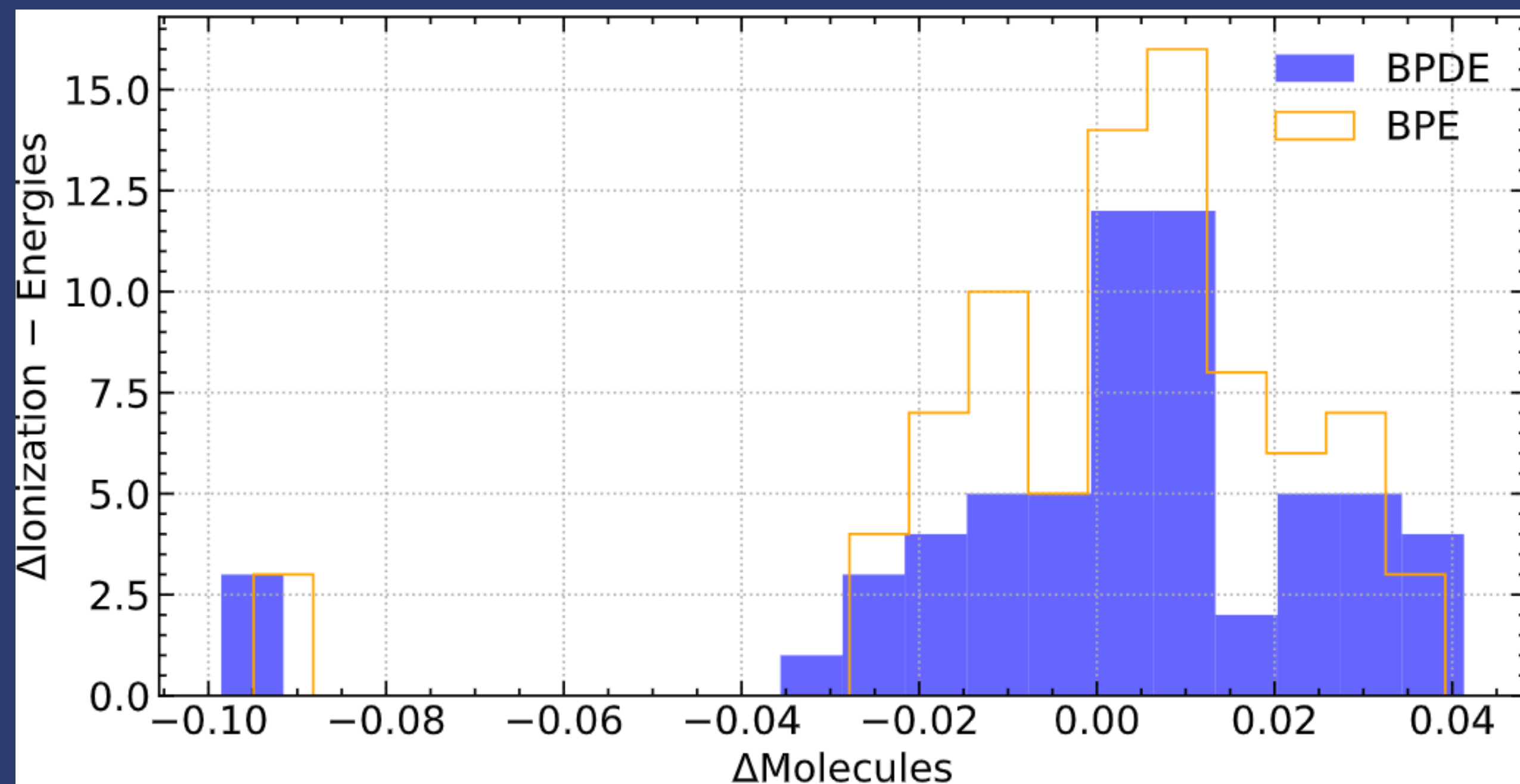


Fig. 9 Distribution of the vertical ionization energies from the quantum circuit simulations and those from the CAS-CI. Adapted from (Sugisaki, 2021).1)

# Singlet–triplet energy gaps

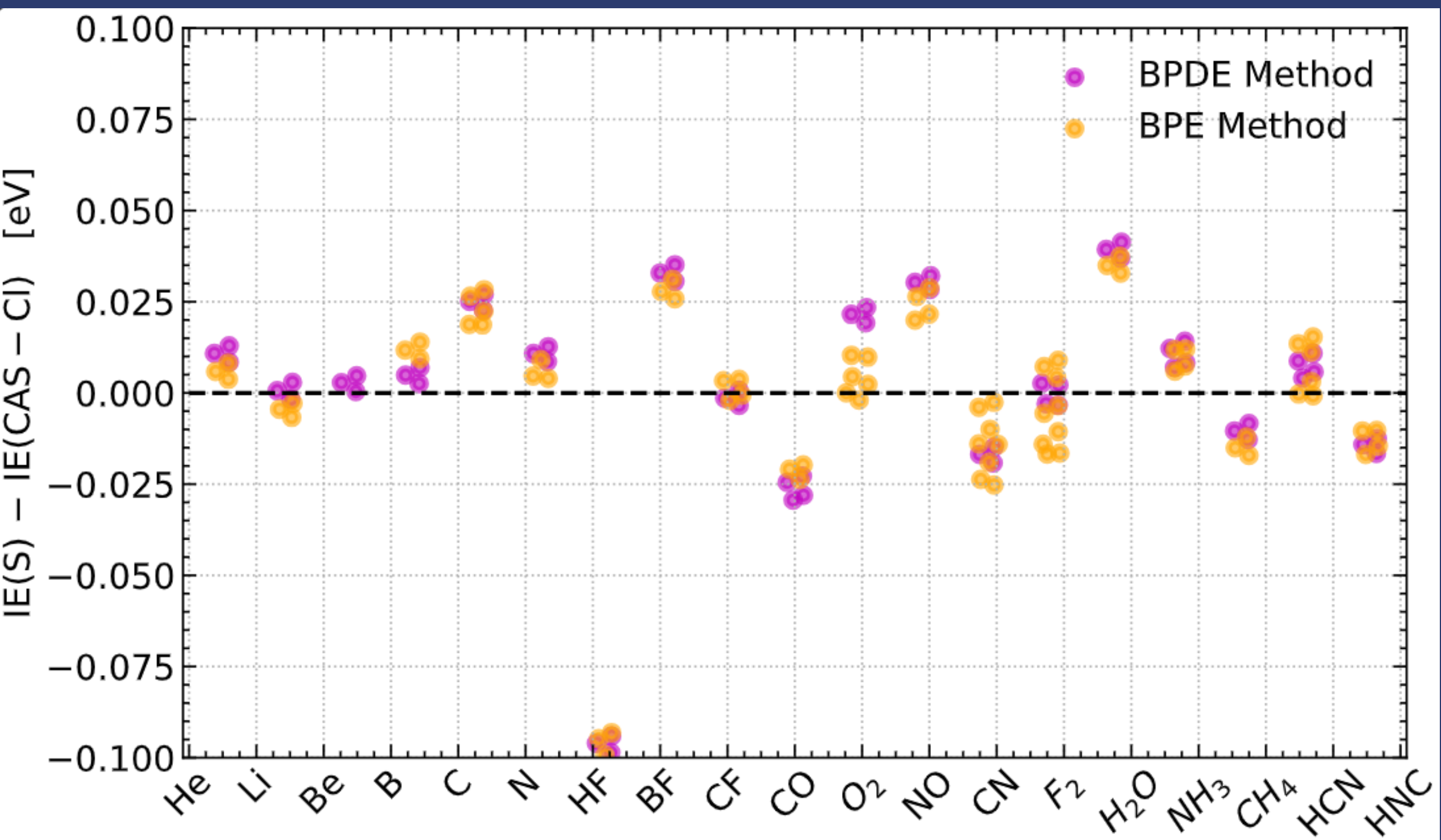


Fig. 10: Differences between the vertical ionization energies from the quantum circuit simulations and those from the CAS-CI calculations for chemical species under study. Adapted from [1].

## Bayesian Phase Difference Estimation (BPDE ) Algorithm

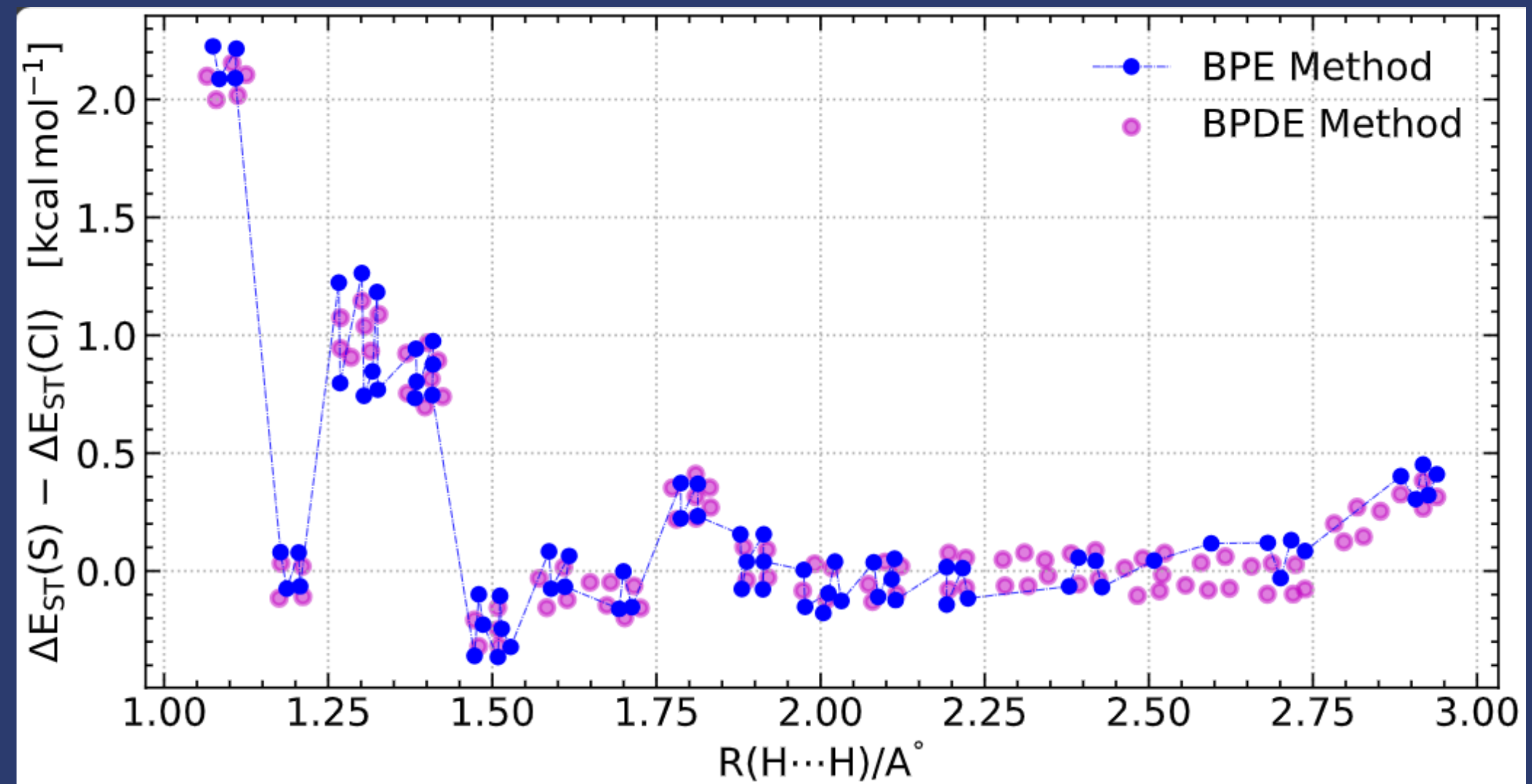


Fig. 11 Differences between the singlet–triplet energy gaps from the quantum circuit simulations and those from the CAS-CI calculations for H<sub>2</sub> molecule with different atom–atom distances. Adapted from [1].

# CONCLUSIONS

Entanglement allows **information to be shared** between particles that are not physically connected. This has implications for quantum computing, as it allows for **faster processing of information**.

One of the most important features of the BPDE in contrast with the BPE, is that BPDE does not dependen on the system size to achieve the convergence

BPDE is also promising in terms of reducing the computational cost of Bayesian optimization.

Not limited range of applications for BPDE and combination to other sophisticated methods for the wave function preparation.

By utilizing entanglement, quantum algorithms are able to perform calculations in parallel, leading to a significant increase in speed and efficiency.

# REFERENCES

- Sugisaki, K., Sakai, C., Toyota, K., Sato, K., Shiomi, D., & Takui, T. (2021). Bayesian phase difference estimation: a general quantum algorithm for the direct calculation of energy gaps. *Physical Chemistry Chemical Physics*, 23(36), 20152-20162.
- Sugisaki, K., Nakazawa, S., Toyota, K., Sato, K., Shiomi, D., & Takui, T. (2019). Quantum chemistry on quantum computers: quantum simulations of the time evolution of wave functions under the  $S^2$  operator and determination of the spin quantum number  $S$ . *Physical Chemistry Chemical Physics*, 21(28), 15356-15361.
- Sugisaki, K., Yamamoto, S., Nakazawa, S., Toyota, K., Sato, K., Shiomi, D., & Takui, T. (2016). Quantum chemistry on quantum computers: a polynomial-time quantum algorithm for constructing the wave functions of open-shell molecules. *The Journal of Physical Chemistry A*, 120(32), 6459-6466.
- Hastings, M. B., Wecker, D., Bauer, B., & Troyer, M. (2014). Improving quantum algorithms for quantum chemistry. arXiv preprint arXiv:1403.1539.

---

# THANK YOU!

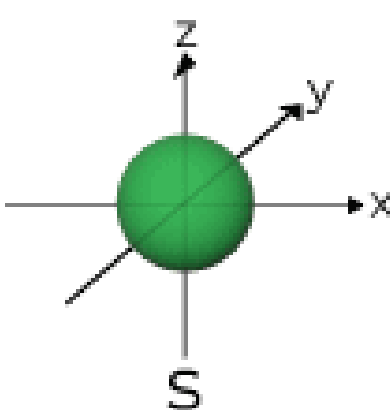
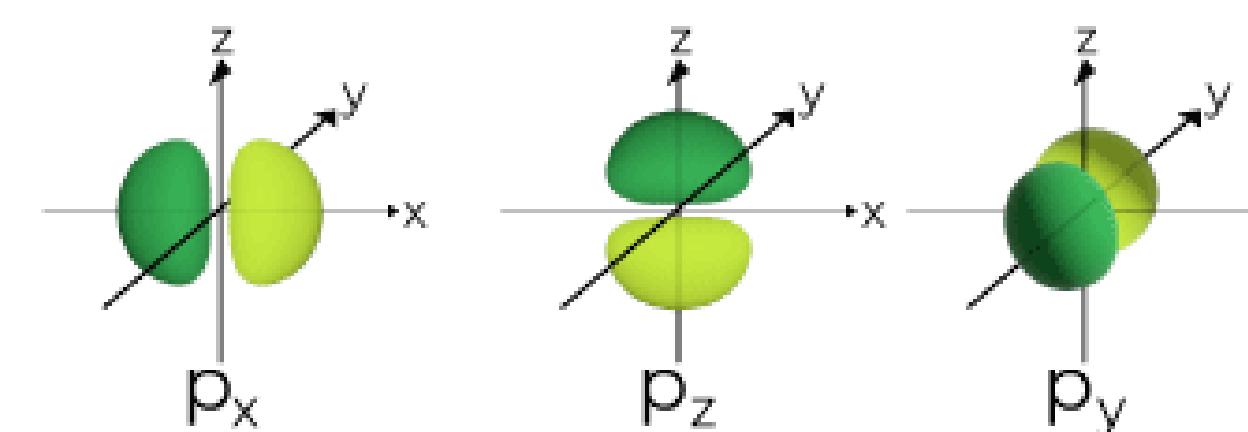
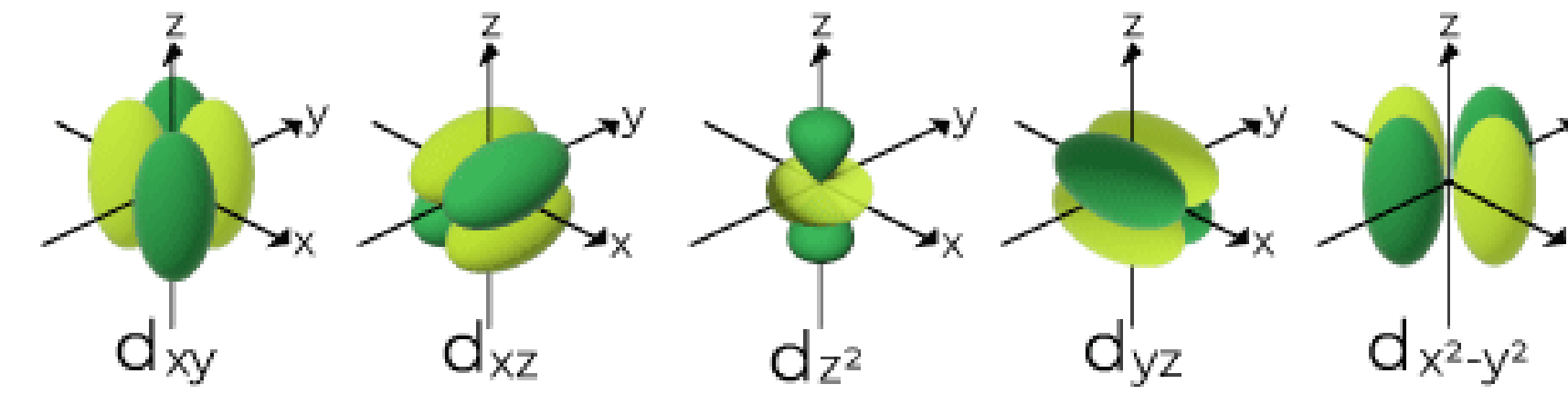
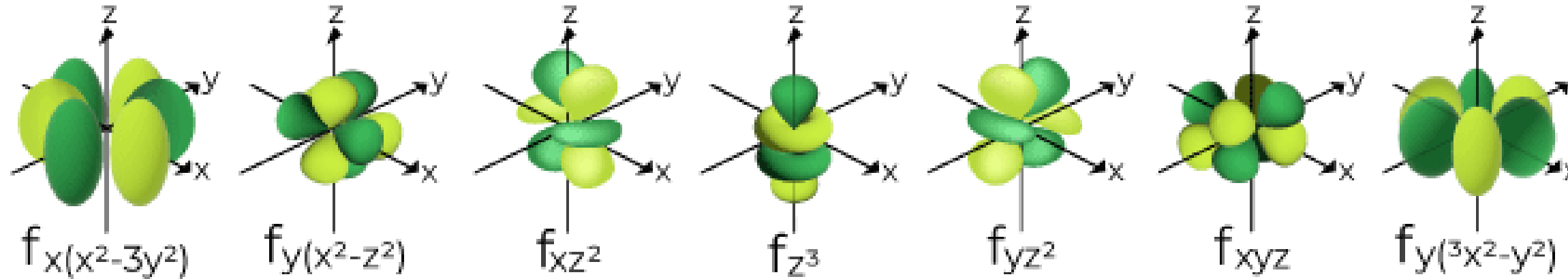
Questions...

# Questions

where  $a_p^\dagger$  and  $a_p$  are fermionic raising and lowering operators satisfying the anticommutation relation  $\{a_p^\dagger, a_q\} = \delta_{pq}$ , the coefficients  $h_{pq}$  and  $h_{pqrs}$  are determined by the discretization that has been chosen, and the sums now run over the number of discretization elements for a single particle. Specifically, if electron  $j$  is represented in a space of spin-orbitals  $\{\phi_p(r_j)\}$  then  $a_p^\dagger$  and  $a_p$  are related to Slater determinants through the equivalence,

$$\langle r_0, \dots, r_{\eta-1} | a_{p_0}^\dagger \cdots a_{p_{\eta-1}}^\dagger | 0 \rangle = \sqrt{\frac{1}{\eta!}} \begin{vmatrix} \phi_{p_0}(r_0) & \phi_{p_1}(r_0) & \cdots & \phi_{p_{\eta-1}}(r_0) \\ \phi_{p_0}(r_1) & \phi_{p_1}(r_1) & \cdots & \phi_{p_{\eta-1}}(r_1) \\ \vdots & \vdots & \ddots & \vdots \\ \phi_{p_0}(r_{\eta-1}) & \phi_{p_1}(r_{\eta-1}) & \cdots & \phi_{p_{\eta-1}}(r_{\eta-1}) \end{vmatrix} \quad (3)$$

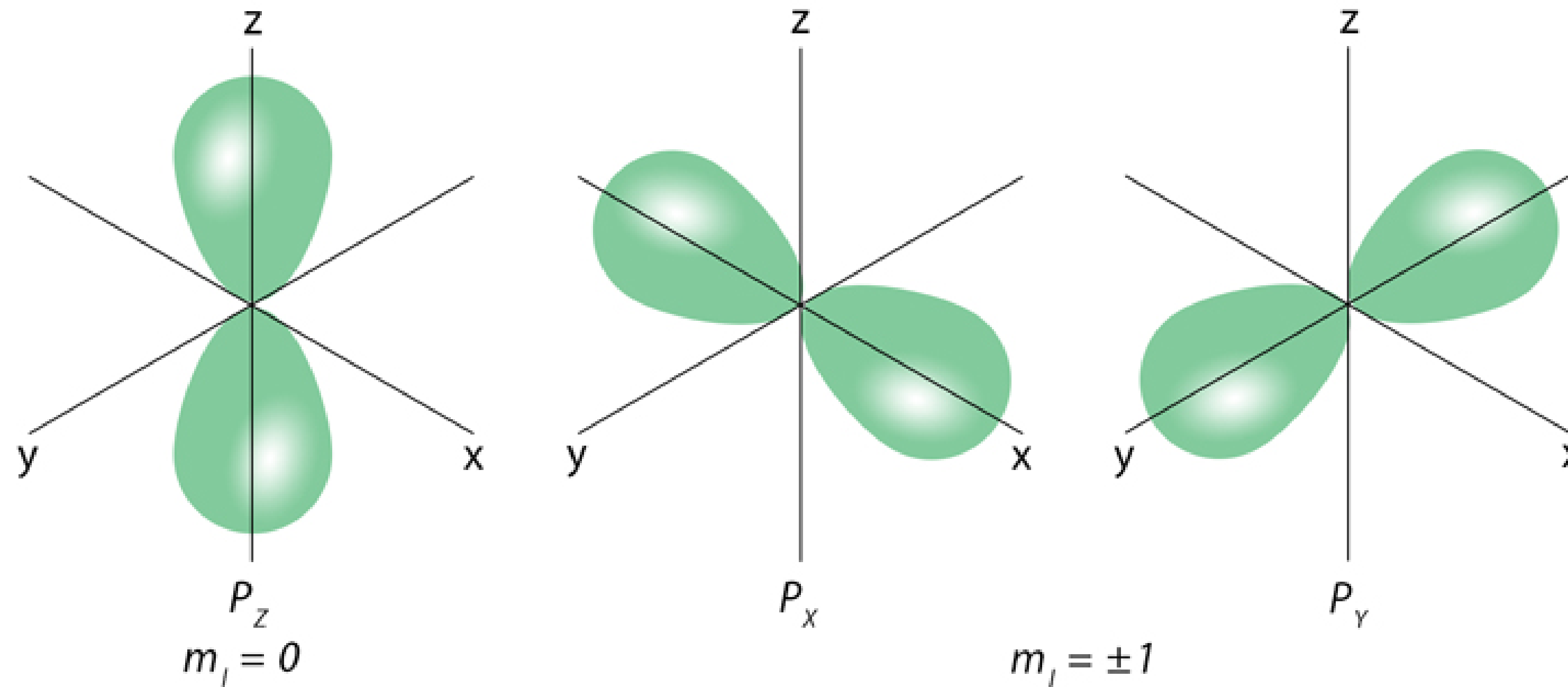
# Questions

S orbital		$n = 1, 2, 3, \dots 7$ $l = 0$ $m = 0$
p orbital		$n = 2, 3, \dots 6$ $l = 1$ $m = 0, \pm 1$
d orbital		$n = 3, 4, \text{and } 5$ $l = 2$ $m = 0, \pm 1, \pm 2$
f orbital		$n = 4$ $l = 3$ $m = 0, \pm 1, \pm 2, \pm 3$

# Magnetic Quantum Number ( $m_l$ )

$m_l$  indicates the orientation of the orbitals

Example:  $p$ -subshell splits into 3 orbitals



# VQE Algorithm

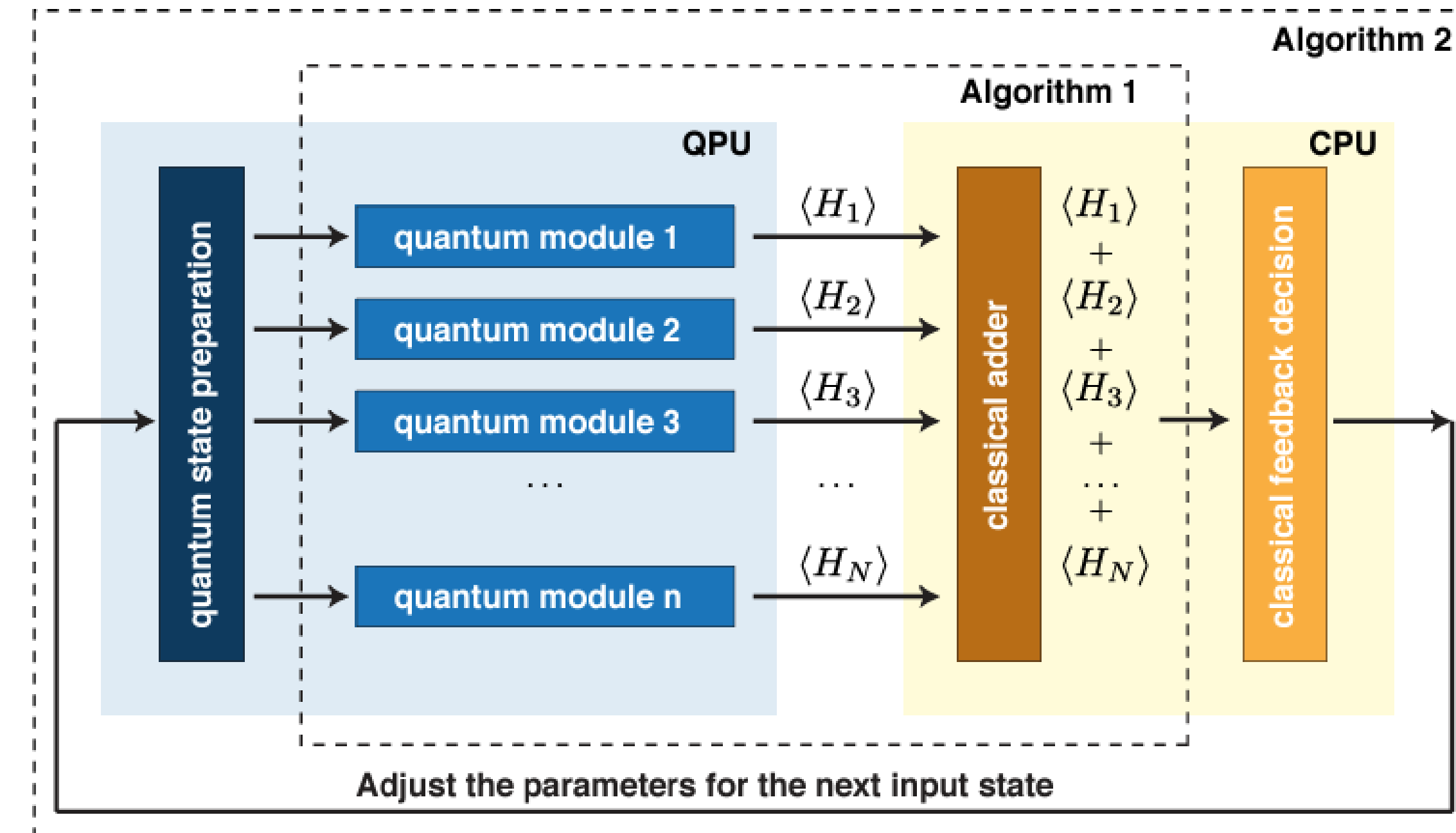
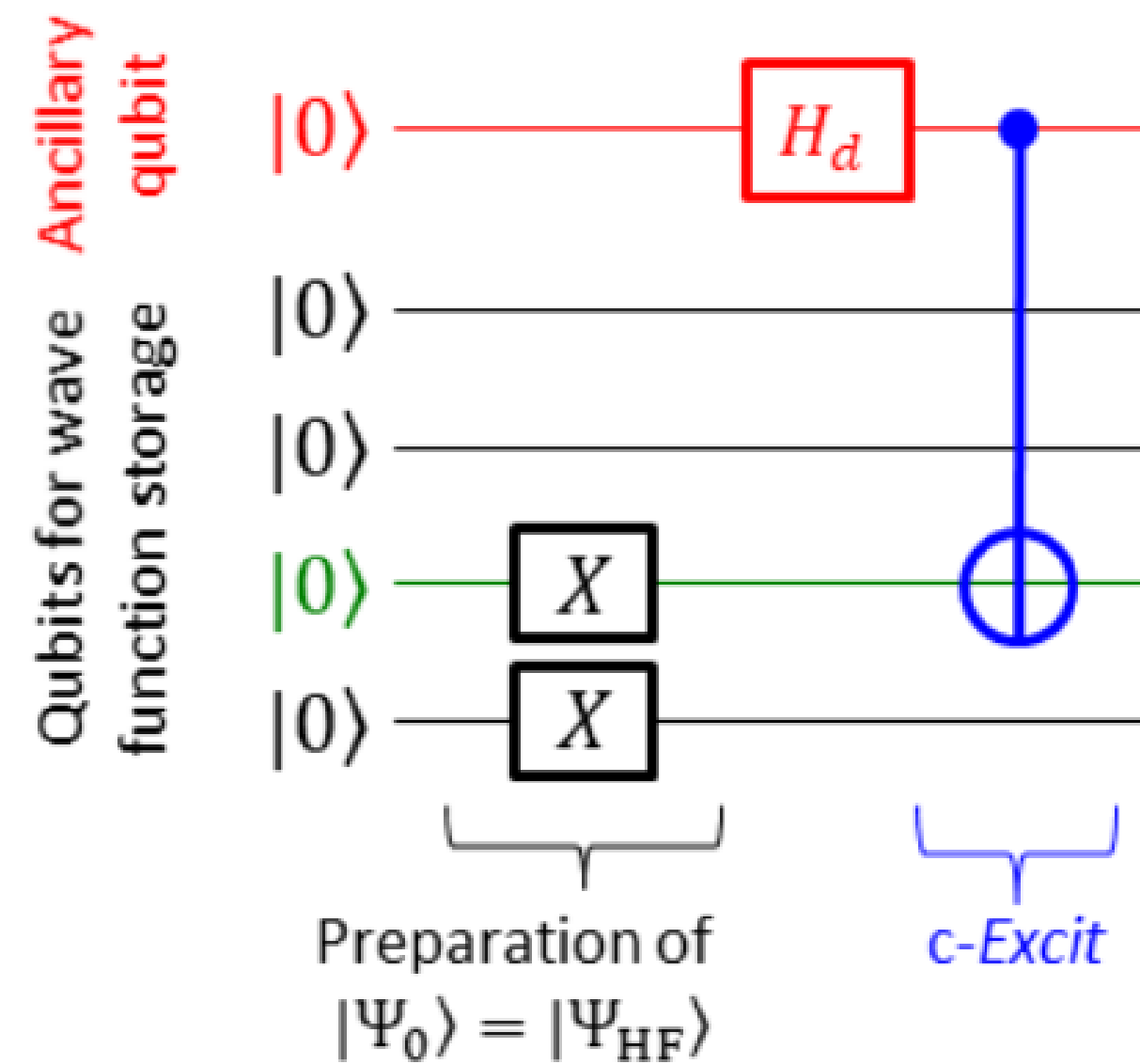
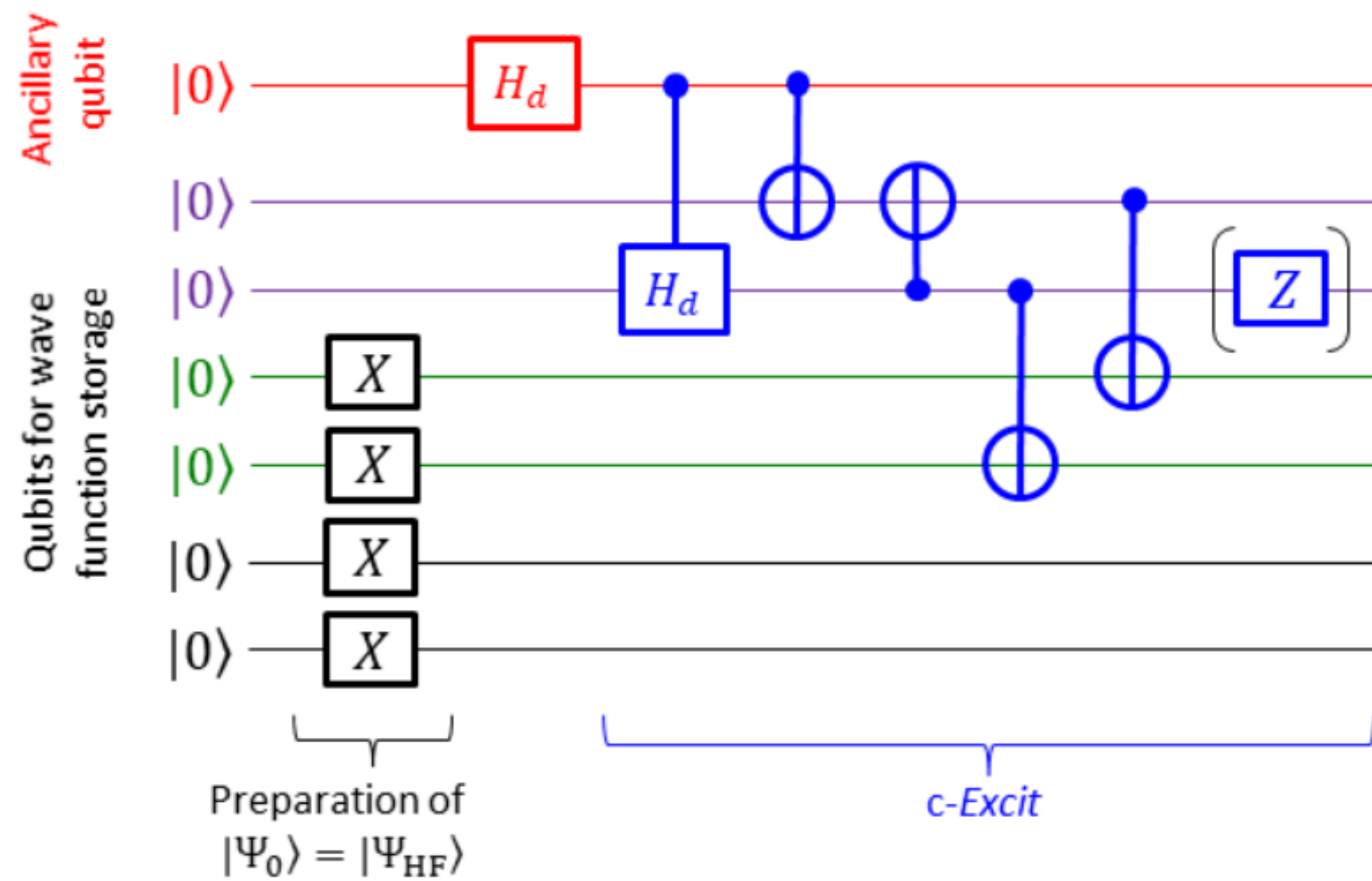


FIG. 1. Architecture of the quantum-variational eigensolver. **Algorithm 1:** Quantum states that have been previously prepared, are fed into the quantum modules which compute  $\langle \mathcal{H}_i \rangle$ , where  $\mathcal{H}_i$  is any given term in the sum defining  $\mathcal{H}$ . The results are passed to the CPU which computes  $\langle \mathcal{H} \rangle$ . **Algorithm 2:** The classical minimization algorithm, run on the CPU, takes  $\langle \mathcal{H} \rangle$  and determines the new state parameters, which are then fed back to the QPU.

# Quantum circuits for the state preparations and controlled-*Excit* operations



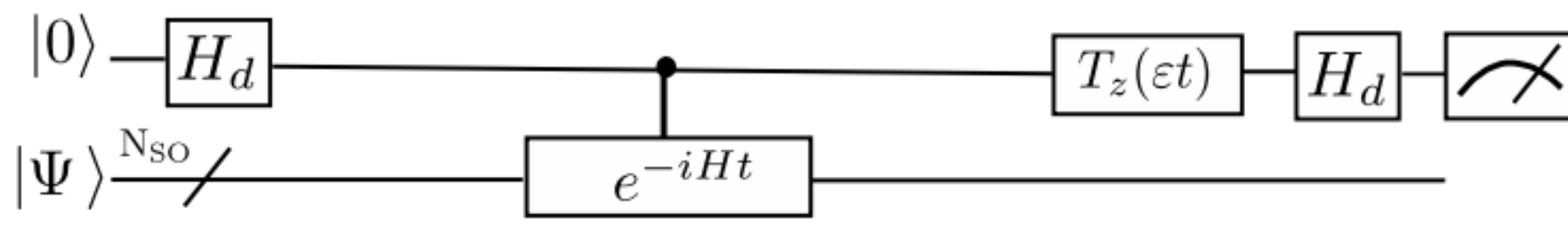
**Fig. S14** An example of the quantum circuit for the wave function preparation and controlled-*Excit* operation in the direct calculation of vertical ionisation energies using the BPDE algorithm. The qubit written in red is the ancillary qubit and that in green is the qubit storing the electron occupancy of the spin orbital of which electron ionisation occurs.



**Fig. S16** An example of the quantum circuit for the wave function preparation and controlled-*Excit* operation in the direct calculation of vertical excitation energies using the BPDE algorithm. The qubit written in red is the ancillary qubit. Electron excitation occurs from the qubits in green to the qubits in purple. The Pauli-Z gate in the parenthesis is required for the calculations of singlet–singlet spin allowed electron excitations, and it should be removed for the calculations of singlet–triplet spin forbidden transitions.

# BPE Algorithm

starts by applying an Hadamard gate ( $H_d$ ) to the ancillary qubit in the top of Fig. 1 (eqn (2)). The next step is for the controlled-time evolution of  $|\Psi\rangle$ . The time evolution operator  $\exp(-iHt)$  is applied to  $|\Psi\rangle$  if and only if the ancillary qubit is in the  $|1\rangle$  state (eqn (3)). After that the  $T_z$  gate is applied to the ancillary qubit to cause the phase shift to the  $|1\rangle$  state (eqn (4)). The following Hadamard gate on the ancillary qubit generates the quantum state in eqn (5).



$$|0\rangle \otimes |\Psi\rangle \xrightarrow{H_d \otimes \text{Id}} \frac{1}{\sqrt{2}}(|0\rangle + |1\rangle) \otimes |\Psi\rangle \quad (2)$$

$$\xrightarrow{c - \exp(-iHt)} \frac{1}{\sqrt{2}}(|0\rangle + e^{-iEt}|1\rangle) \otimes |\Psi\rangle \quad (3)$$

$$\xrightarrow{T_z(\varepsilon t) \otimes \text{Id}} \frac{1}{\sqrt{2}}\left(|0\rangle + e^{-i(E-\varepsilon)t}|1\rangle\right) \otimes |\Psi\rangle \quad (4)$$

$$\begin{aligned} &\xrightarrow{H_d \otimes \text{Id}} \frac{1}{2}\left(1 + e^{-i(E-\varepsilon)t}\right)|0\rangle \otimes |\Psi\rangle \\ &+ \frac{1}{2}\left(1 - e^{-i(E-\varepsilon)t}\right)|1\rangle \otimes |\Psi\rangle \end{aligned} \quad (5)$$

The probability to obtain the  $|0\rangle$  state in the measurement of the ancillary qubit,  $P(0)$ , is calculated as in eqn (6).

$$P(0) = \frac{1}{2}[1 + \cos\{(E - \varepsilon)t\}] \quad (6)$$

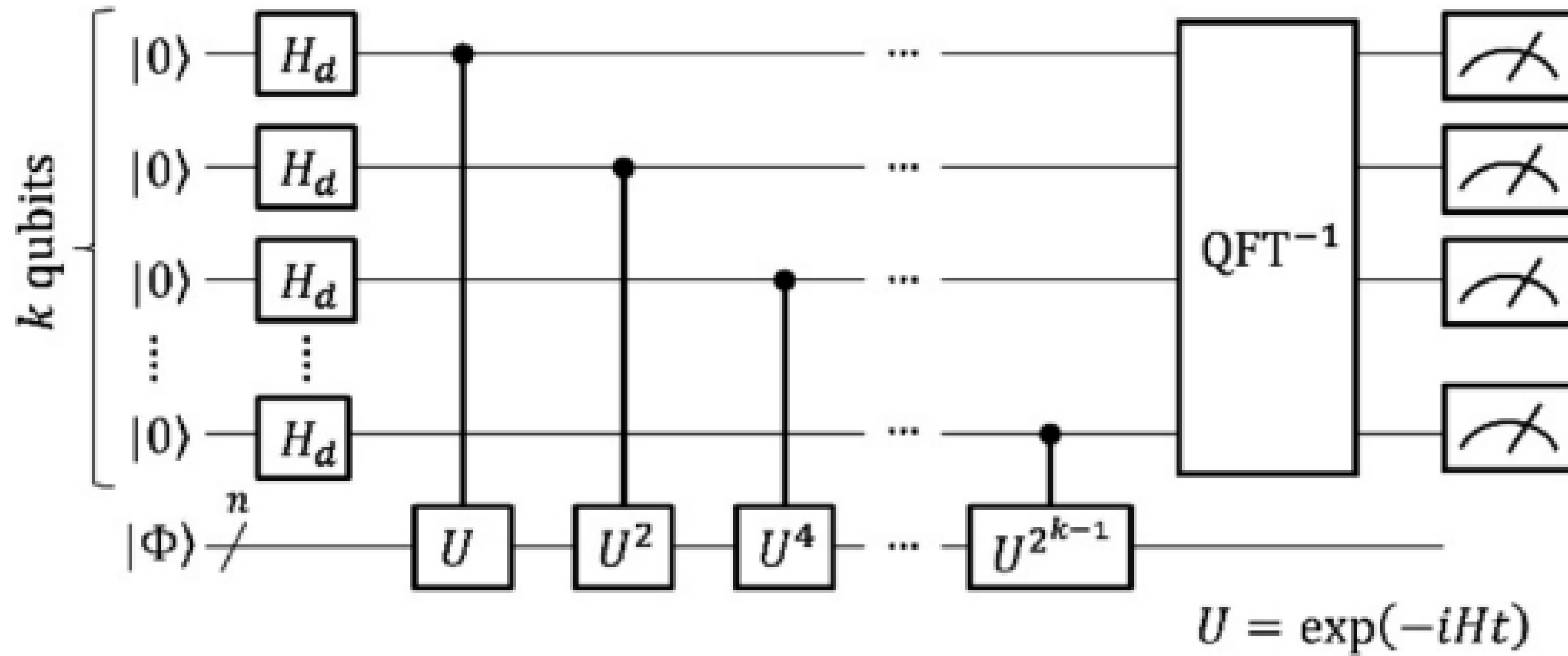


**Fig. 1** A quantum circuit of the quantum phase estimation-based full-CI calculations.